Electronic Supplementary Material (ESI) for Nanoscale Advances.

Supporting Information: Weaving Nanostructures with Site-Specific Ion Induced Bidirectional Bending

Vivek Garg,[a, b, c], Tsengming Chou[d], Amelia Liu[e], Alex De Marco[f], Bhaveshkumar Kamaliya[a, c, g], Shi Qiu[c], Rakesh G. Mote[*b], and Jing Fu[*c]

[a]*IITB-Monash Research Academy, Indian Institute of Technology Bombay, Powai, Mumbai 400076, India.*

[b]*Department of Mechanical Engineering, Indian Institute of Technology Bombay, Powai, Mumbai 400076, India*

[c]*Department of Mechanical and Aerospace Engineering, Monash University, Wellington Road, Clayton, Victoria 3800, Australia*

[d]*Laboratory of Multiscale Imaging, Stevens Institute of Technology, Hoboken, NJ 07030, USA*

[e]*Monash Centre for Electron Microscopy, Monash University Clayton, VIC 3800, Australia*

[f]*Department of Biochemistry and Molecular Biology, Monash University, Clayton, VIC 3800, Australia*

[g]*Department Physics, Indian Institute of Technology Bombay, Powai, Mumbai 400076, India*

*E-mail: rakesh.mote@iitb.ac.in and jing.fu@monash.edu

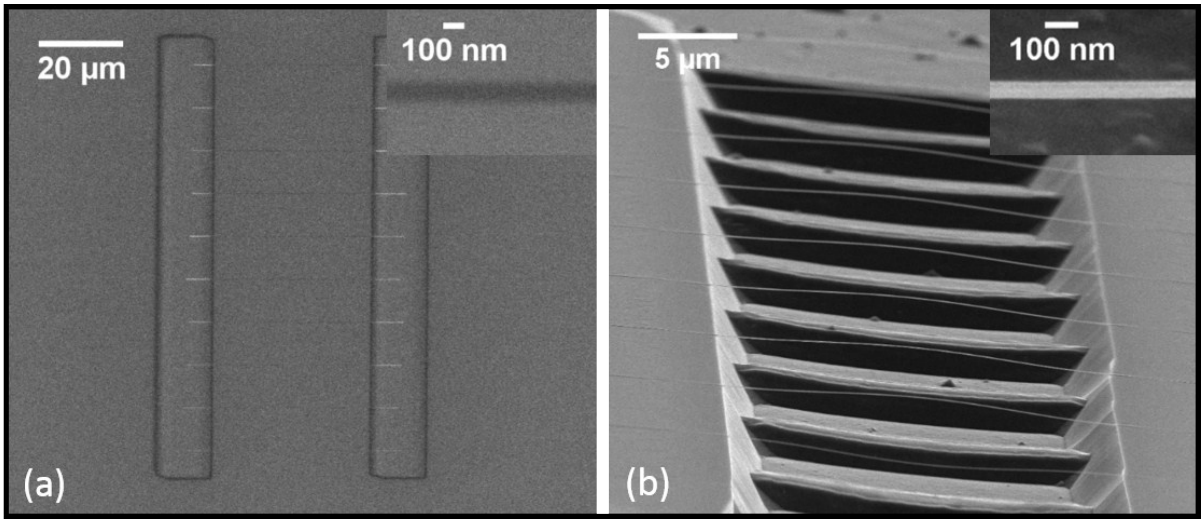

Figure S1: Si nanowires, SEM image of - (a) FIB implanted line profiles over two contact pads for fabrication of suspended Si NWs, inset includes a high resolution SEM image for demonstration of a typical implantation profile; (b) fabricated NWs, inset shows a high resolution SEM image of the NW

Fabrication of Si nanowires was facilitated by FIB assisted implantation and wet chemical bulk structuration. Improved etching resistance of FIB induced amorphous Si (a-Si) in contrast to crystalline Si (c-Si) is employed as a mask and the Si NWs are fabricated in a top-down manner. The amorphization of Si under ion irradiation occurs when the free energy of the damaged crystalline phase gets higher than the amorphous phase [1]. Figure S1 (a) displays the SEM image of FIB line implantation profile over two parallel rectangles with a comparatively higher implantation dose. The rectangles implanted with a higher ion dose work as contact pads to expedite the fabrication of suspended NWs on a Si substrate. The inset in figure S1 (a) also includes a high resolution SEM image of FIB line implantation profile. The wet etching of FIB implanted Si substrate with KOH solution leads to the development of Si NWs, which are suspended over two parallel rectangles as shown through SEM image in figure S1 (b). A representative SEM image of fabricated Si NWs with a typical diameter/width of 100 nm through bulk structuration of Si is shown in the inset of

figure S1 (b). The fabricated NWs demonstrate high fidelity and the technique can be employed for realization of ultra-long aspect ratio suspended NWs for controlled manipulation of nanostructures offering a variety of 3-dimensional (3D) configurations, extending the FIB nanofabrication capabilities [2,3]. These NWs are employed for study and characterization of in-situ FIB induced bending for controlled nano-manipulation.

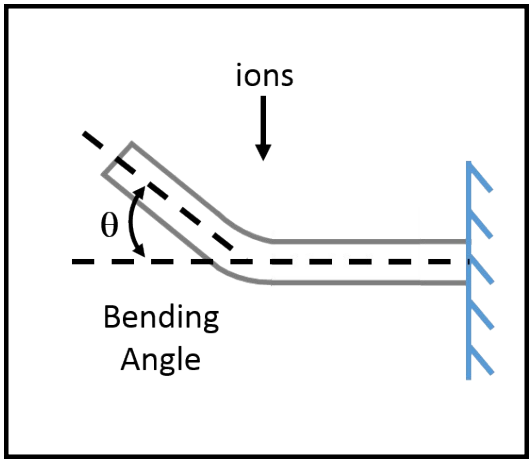

Figure S2: Schematic diagram showing the incident FIB on NW cross-section and the NW bending angle

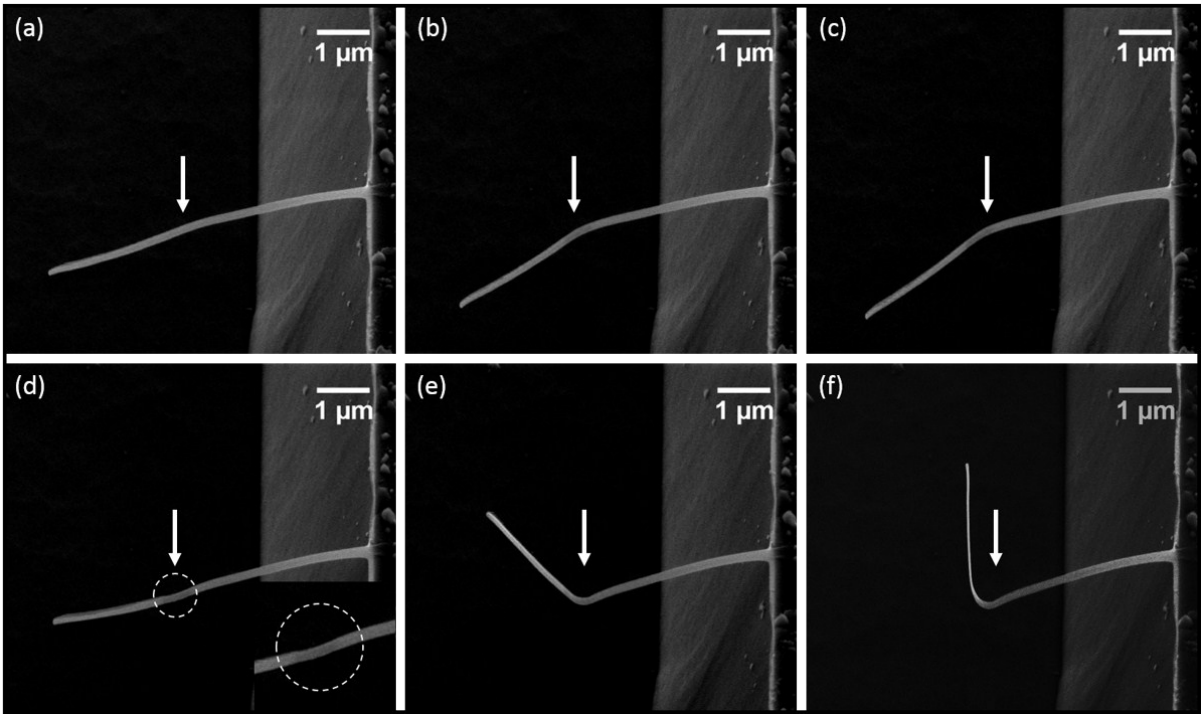

Figure S3: A series of representative SEM images acquired at successive time-intervals during ion-beam irradiations at ion doses of (a) 3.4×10^{14}, (b) 5.2×10^{14}, (c) 6.9×10^{14}, (d) 1.7×10^{15}, (e) 2.8×10^{15}, and (f) 3.1×10^{15} ions/cm^2 and acceleration voltage 30 kV, Observation of downward (a)-(c) and upward bending (d)-(f). The NW cross-section showing Si sputtering/erosion during upward bending is highlighted with a circle and magnified SEM image in (d)

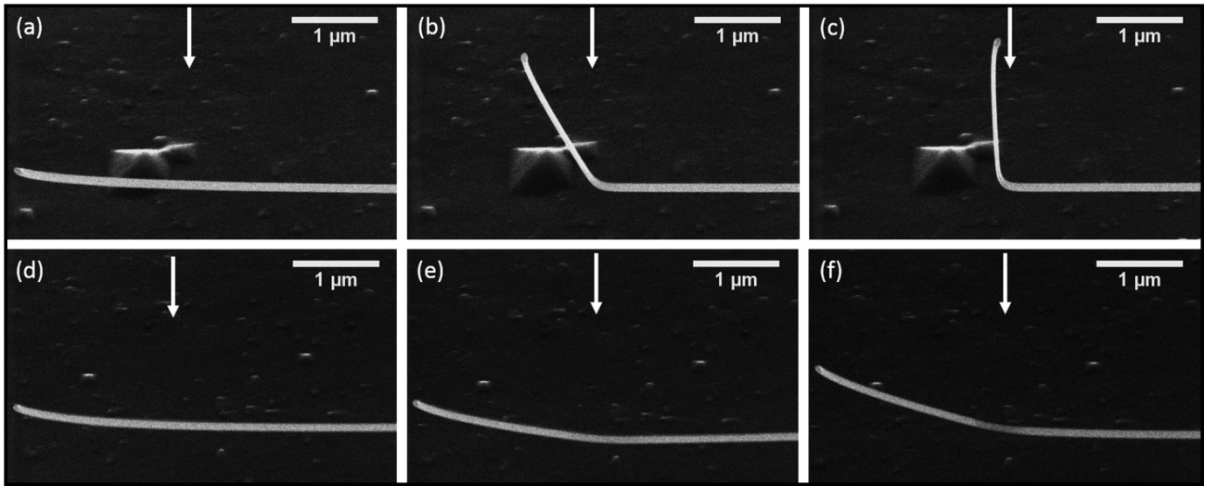

Figure S4: Experiments at medium 16 kV acceleration voltage and ion dose of (a) 1.1×10^{14}, (b) 7.8×10^{15}, (c) 2.0×10^{16} ions/cm^2; low 2 kV acceleration voltage and ion dose of 2 kV (d) 1.1×10^{14}, (e) 3.1×10^{16}, (f) 1.8×10^{17} ions/cm^2. A series of representative SEM images acquired at successive time-intervals during respective ion-beam irradiations are shown. (a)-(c) upward bending and NW is aligned in the ion beam incidence direction (d)-(f) Upward bending, however NW is not aligned completely along the beam incidence direction at low kV.

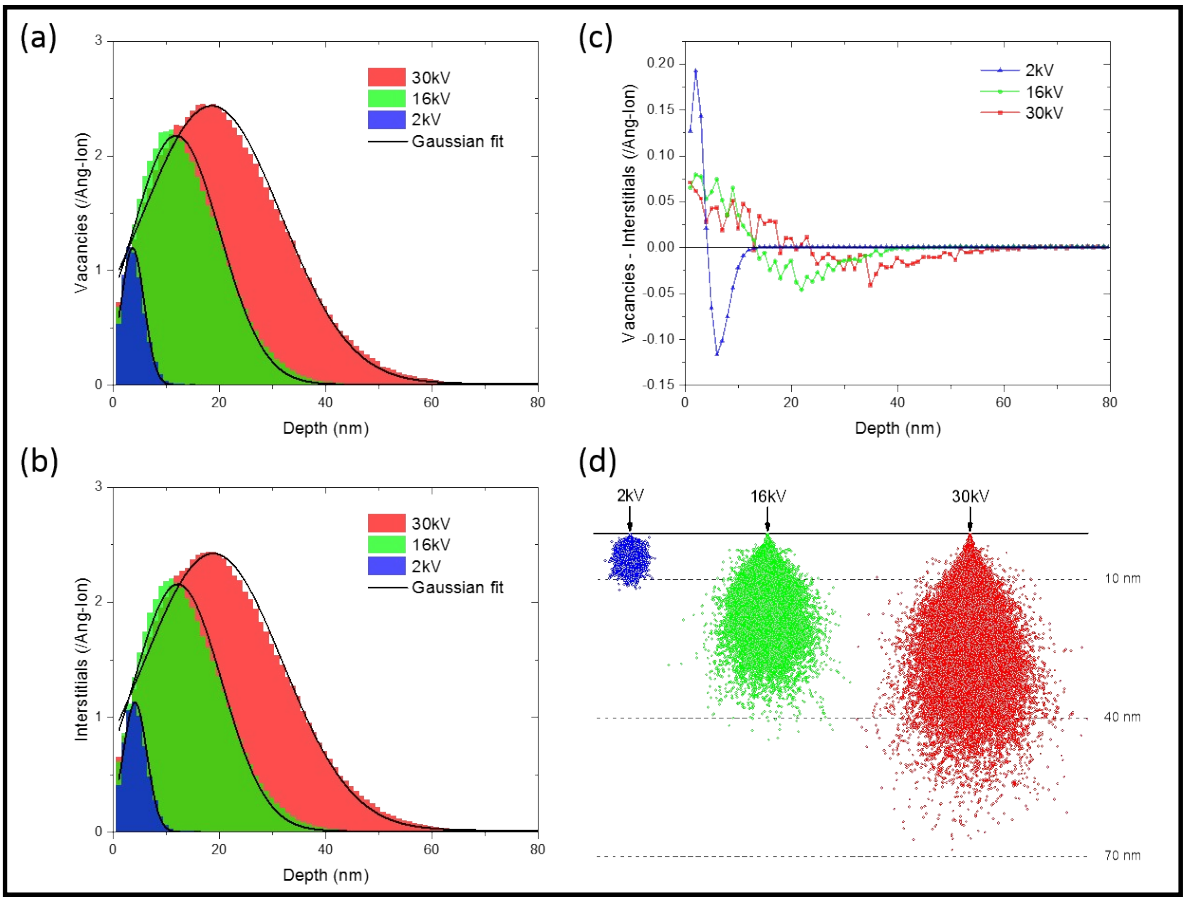

Figure S5: Bending of Si NWs- effect of FIB irradiations on Si: (a) Vacancy; (b) interstitial distributions in Si irradiated with 30, 16, and 2 kV Ga ions; (c) the difference of vacancies and interstitials/Ang-Ion (d) trajectories and interaction volume of incident Ga ions caused by Ga ions in 80 nm thick Si substrate calculated with Monte Carlo SRIM simulations

SRIM CALCULATIONS

The Ga ions undergo electronic and nuclear stopping through collisions with electrons and Si nuclei before coming to rest. Due to these collisions, few Si atoms are ejected from their lattice positions as primary knock on atoms, if the energy transferred through Ga ions is more than displacement energy of Si (~15 eV) [4], and create a Frenkel pair. These primary knock on atoms leave the vacancies at their original lattice position, can further interact with lattice atoms and produce a cascade of atomic displacements, before forming an interstitial atom.

Thus, a single Ga ion develops a complete collision cascade, forming point defects (vacancies and interstitials) and Ga implantation in the crystal lattice. However, if the threshold energy is lower, only local heating occurs, known as thermal spike regime. The thermal spike regime of the cascade can cause significant melting and formation of amorphous pockets in the collision cascade, which contain more displaced atoms than calculated with binary collisions [1,5]. The formation of vacancies and interstitials distributions in Si is calculated. There is a slight difference between the number of vacancies and interstitials formation in the Si target. Vacancy formation in the Si corresponds to volumetric contraction. The volumetric contraction is responsible for generation of tensile stress. In contrast the interstitials distribution of ion leads to volume expansion, which will give rise to compressive stresses in the target [6]. The comparison of difference in vacancies and interstitials at low and high kV reveals the relative location of vacancy/interstitials excess along the target depth as a result of Ga FIB bombardment.

The total number of atomic displacements/Si damage is calculated by vacancy and replacement collisions as follows:

Displacements=Vacancies + Replacement collisions

The total numbers of vacancies are calculated using SRIM simulations and according to following:

Vacancies=interstitials + atoms exited from Si

The Si recoil atoms calculated from SRIM simulations are the sum of replacement collisions and interstitials, thus the number of interstitials can be calculated as follows:

Interstitials= Si recoils – replacement collisions

The difference between vacancies and interstitials is plotted in figure S5 (c) for better visualization and understanding the interplay effects on bending phenomenon. The positive values in the plot of figure S5 (c) represent vacancy excess, while negative values indicate interstitials excess in Si caused by Ga ions.

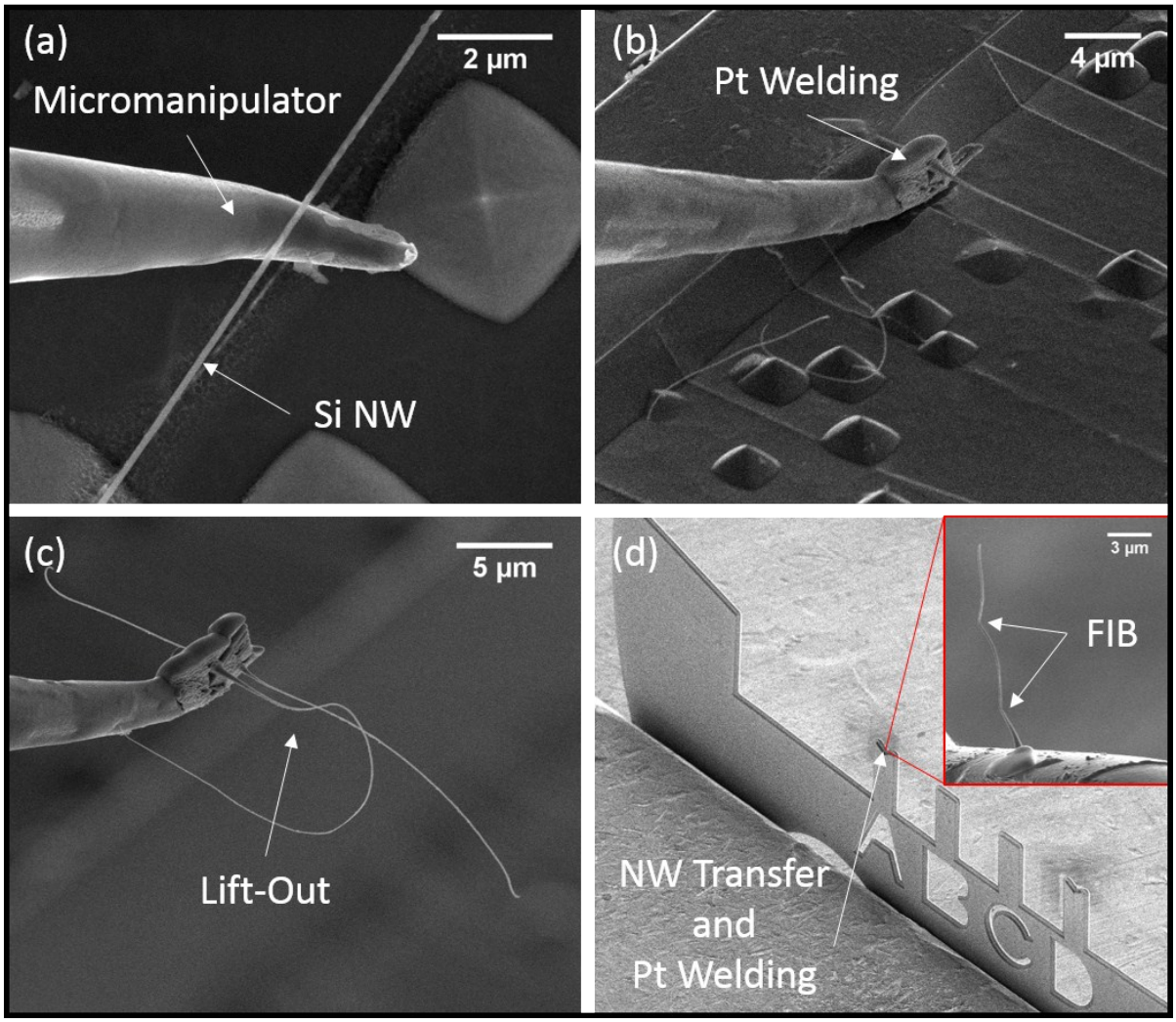

Figure S6: Si NW TEM sample preparation for microstructural characterization: SEM images showing (a) Kleindiek micromanipulator tip positioned below the NW on Si substrate; (b) Pt welding to fix NW over micromanipulator; (c) lift-out from the substrate; (d) NW transfer to TEM grid and Pt welding of NW to the grid, inset in (d) shows a transferred NW which is welded with Pt to TEM grid. The transferred NW is further exposed to FIB for ion induced bending characterization over two cross-sections as depicted in inset of (d)

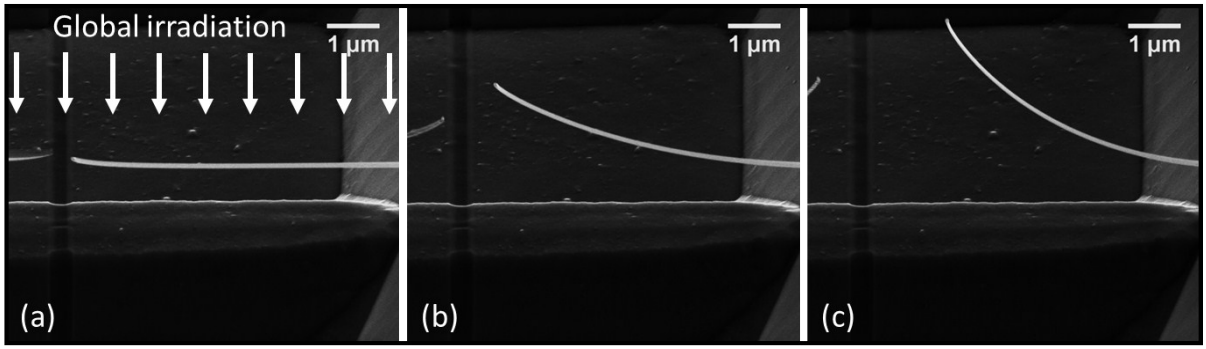

Figure S7: Global ion irradiation: (a)-(c) A series of representative SEM images acquired at successive time-intervals during global ion-beam irradiations showing upward bending at 30 kV in contrast to bidirectional bending through local ion irradiation at 30 kV (figure S3)

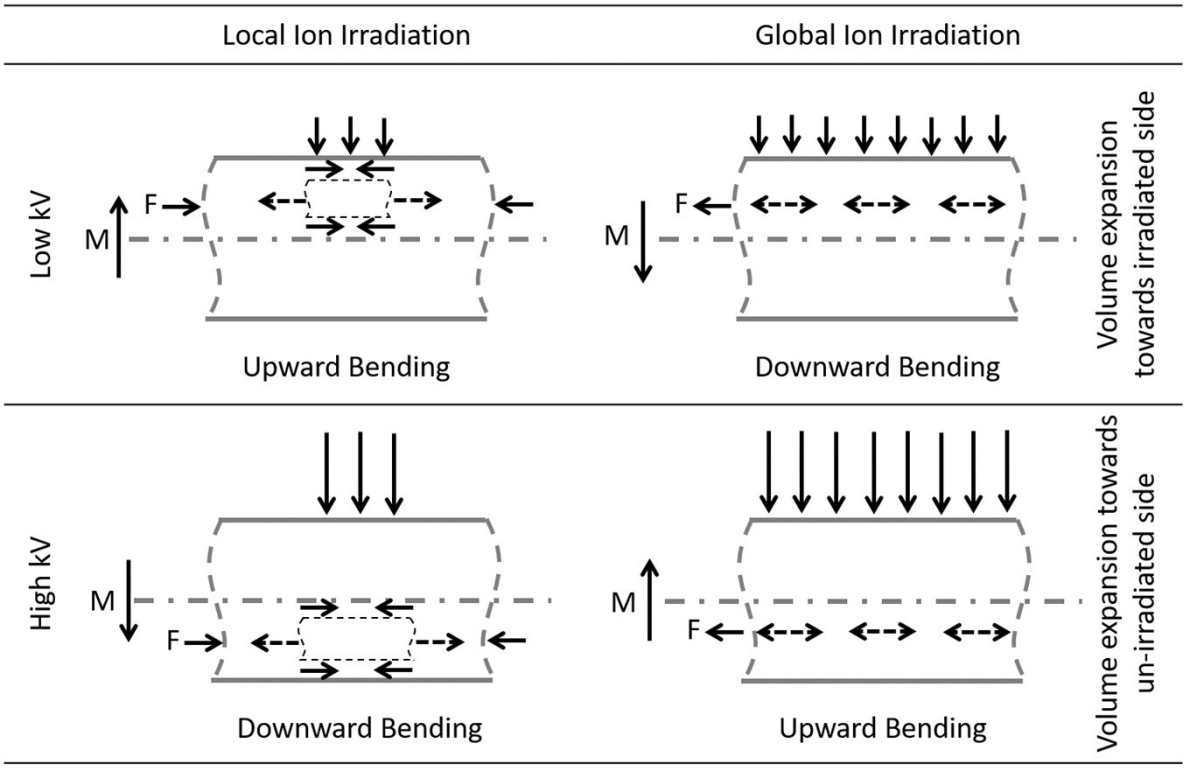

Figure S8: Ion irradiation induced bending of nanostructures: Local vs global ion irradiation

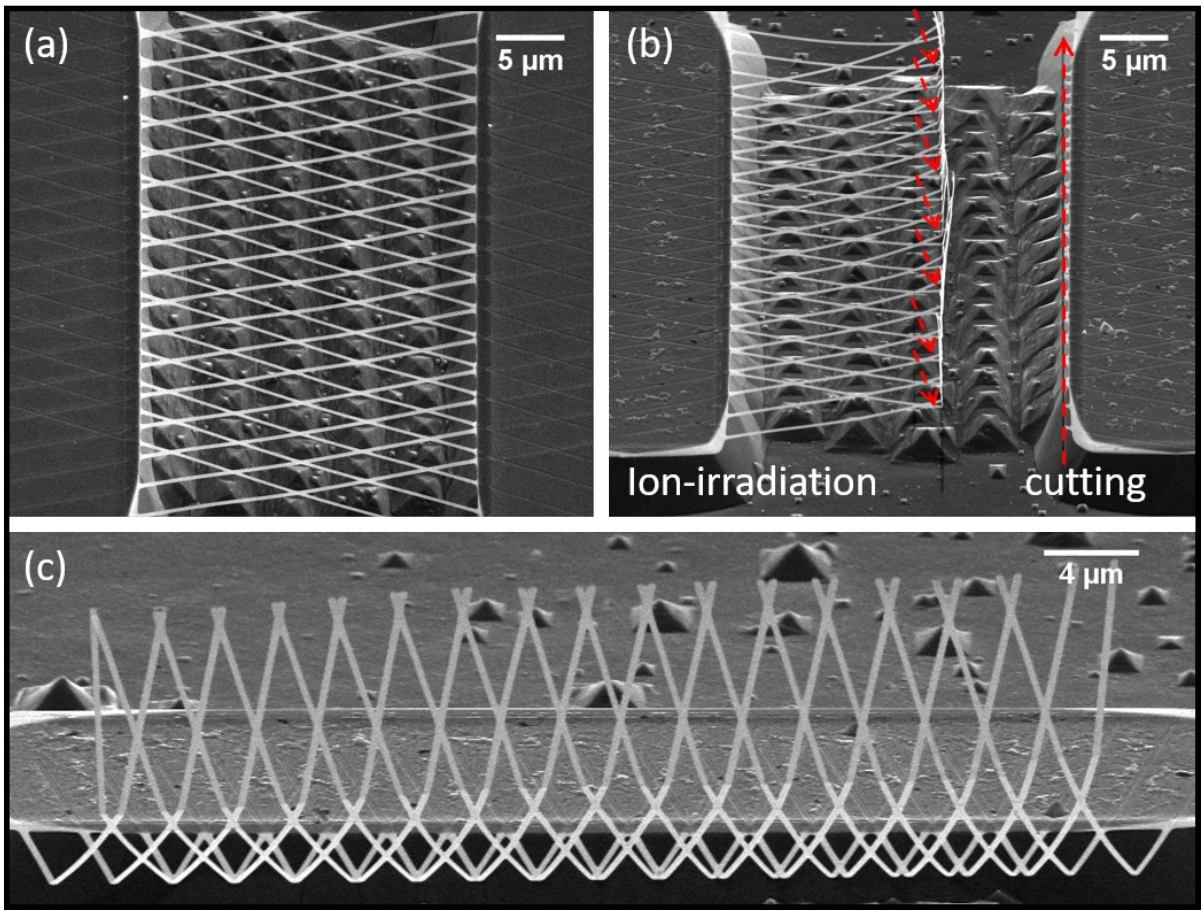

Figure S9: Weaving nanostructures: controlled manipulation and bending of suspended Si mesh structure. SEM image in (a) shows the fabricated Si mesh structure suspended over two contact pads. The suspended mesh is cut with FIB and subsequently bent via ion irradiations as shown through SEM image in (b). SEM image in (c) shows the fabricated nanostructure after manipulation with FIB

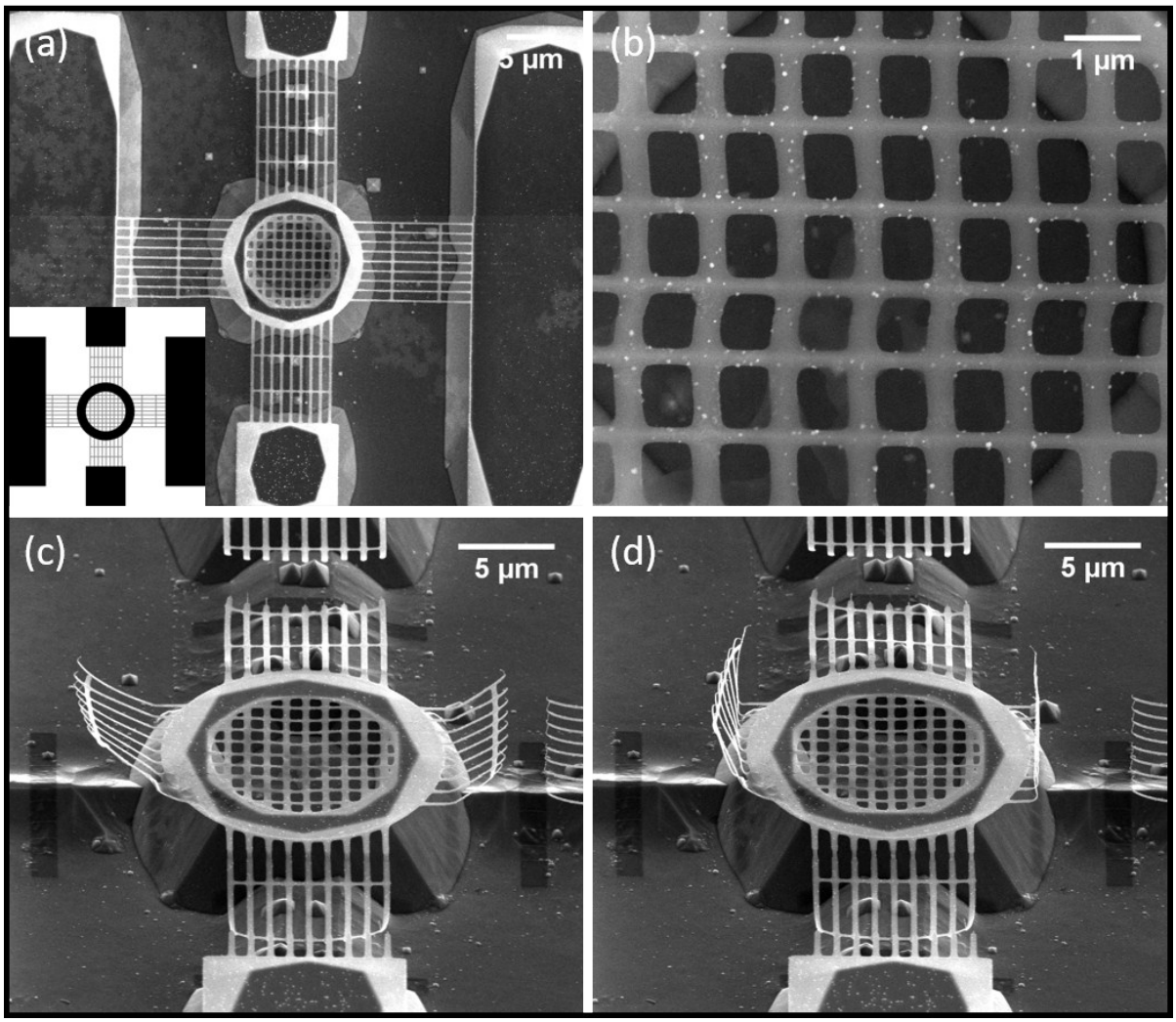

Figure S10: Design and fabrication of bacteria lobster trap: (a), (b) SEM images of fabricated mesh structure, with inset in (a) showing the bitmap image used for fabrication; (c), (d) showing subsequent FIB cutting and in-situ folding

REFERENCES

1 L. Pelaz, L. A. Marqués and J. Barbolla, *Journal of Applied Physics*, 2004, **96**, 5947–5976.
2 V. Garg, R. G. Mote and J. Fu, *Advanced Materials Technologies*, 2018, **3**, 1800100.
3 V. Garg, R. G. Mote and J. Fu, in *Precision Product-Process Design and Optimization*, Springer, Singapore, 2018, pp. 189–209.
4 J. W. Corbett and G. D. Watkins, *Phys. Rev.*, 1965, **138**, A555–A560.
5 T. Diaz de la Rubia and G. H. Gilmer, *Phys. Rev. Lett.*, 1995, **74**, 2507–2510.
6 C. Borschel, R. Niepelt, S. Geburt, C. Gutsche, I. Regolin, W. Prost, F.-J. Tegude, D. Stichtenoth, D. Schwen and C. Ronning, *Small*, 2009, **5**, 2576–2580.